Coexistence of stationary and traveling waves in reaction-diffusion-advection systems

Razvan A. Satnoianu
Department of Mathematics, City University London, London EC1V 0HB, United Kingdom
(Received 7 November 2002; revised manuscript received 20 May 2003; published 12 September 2003)

The flow- and diffusion-distributed structures (FDS) and the differential-flow instability (DIFI) are mechanisms that give rise to static and traveling waves in reactive flows with general, species-dependent transport terms. Here we consider a general framework which supports the simultaneous existence of FDS and DIFI patterns. We study the necessary conditions for each instability in general and compare them in order to derive their connection. The interaction between FDS and DIFI patterns gives rise to interesting wave behavior including stationary, upstream, and downstream traveling waves as well as an interesting regime where stationary and traveling waves coexist.

DOI: 10.1103/PhysRevE.68.032101 PACS number(s): 82.20.−w

I. INTRODUCTION

Over the last decade a wide variety of spatiotemporal structures have been documented in systems of reaction-diffusion-advection (RDA) equations. Prominent examples, such as traveling and stationary waves are known to occur via the flow- and diffusion-distributed structures (FDS) [1] and differential-flow instability (DIFI) scenarios [2,11]. We recently extended the theory to open reactive flows with a fixed inflow boundary condition and proposed a general scenario that gives rise to stable stationary, space periodic patterns [1,3]. The mechanism of flow- and diffusion-distributed structures (FDS) is robust [3] and has none of the limitations of the Turing scenario [4]. Furthermore, in the limit of vanishing flow it recovers the Turing mechanism. The interaction of FDS and Turing instabilities was studied in [3]. The particular case of stationary waves in an oscillatory medium with equal flow and diffusion rates was proposed theoretically in [5] and was subsequently demonstrated experimentally in [6]. Other recent theoretical studies modeling the FDS waves have been reported using the classical model for a cross-flow reactor [7] and the Oregonator [8] and Brusselator [9] models. Those papers have presented scenarios for complex spatiotemporal patterns in such systems.

Similarly, it was recently shown that traveling waves arise when the boundary condition at the inflow region is time periodic [10]. It was shown that the gene-expression waves that precede the formation of somites (the precursors of vertebrae) in chick and mouse embryos arise by a FDS mechanism that involves axial growth, coupled with periodic forcing at the growth zone. The connection between developmental biology and open flows comes from the recognition of the equivalence of axial growth and open flow [10].

In this Brief Report we discuss the link between DIFI and FDS and observe an interesting wave behavior arising from the interaction of the two. The analytical results are derived in Sec. II. In Sec. III the results are illustrated numerically for the cubic autocatalator scheme [11]. A subsequent study of the Oregonator system [12], FitzHugh-Nagumo [13], and the chlorine iodide malonic acid (CIMA) reaction [14] models suggests that the present scenario is quite universal. These results will be presented elsewhere [15].

II. REACTION-DIFFUSION-ADVECTION SYSTEMS WITH GENERAL DIFFUSION AND FLOW RATES

We consider a general reaction-diffusion-advection model that allows for arbitrary differential rates of flow and diffusive transport of the key reactive species. This RDA system admits a variety of instabilities, among them FDS [1,3,5,6], DIFI (or differential-flow) [2,11], and Turing [4] instabilities. Here we are interested in the possible coexistence and interacting behavior of FDS and DIFI patterns. The general equations for a one-dimensional spatial domain are

$$\frac{\partial a}{\partial t}=\delta\frac{\partial^2 a}{\partial x^2}-\phi\frac{\partial a}{\partial x}+f(a,b), \tag{2.1}$$

$$\frac{\partial b}{\partial t}=\frac{\partial^2 b}{\partial x^2}-r\phi\frac{\partial b}{\partial x}+g(a,b), \tag{2.2}$$

where a, b, t, and x are the dimensionless concentrations, time, and distance along the reactor ($t>0$, $0<x<\infty$). As the domain is semi-infinite the effects of the outflow boundary are negligible. $\delta=D_a/D_b$ is the ratio of diffusion coefficients of species a and b. r is the ratio of the advection rates of the two species, or the *differential-flow parameter*. ϕ is the dimensionless flow velocity of b. Without any loss of generality we assume that $\phi>0$. From now on we shall consider that the parameters r and δ are independent and take the advection rate ϕ as our bifurcation parameter. For the reaction terms we chose the cubic autocatalator model [11]

$$f(a,b)=\mu-ab^2, \quad g(a,b)=ab^2-b. \tag{2.3}$$

This ordinary differential equation (ODE) system has a single steady state $S=\{a_s=1/\mu,\ b_s=\mu\}$, for all $\mu>0$. S is temporally unstable (for the ODE system) for any $\mu\leqslant 1$ and temporally stable for $\mu>1$ [3,11]. At $\mu=1$ there is a supercritical Hopf bifurcation with periodic solutions existing in the region $\mu_0=0.9003\leqslant\mu\leqslant 1=\mu_1$. We now analyze the conditions for forming nonuniform structures borne out from small perturbations to the temporally stable uniform steady state S. To do so put

$$a=a_s+A, \quad b=b_s+B, \tag{2.4}$$

where $|A| \ll a, |B| \ll b$. We do the calculations in general and later we specialize the results for the kinetics (2.3). Substituting Eq. (2.4) into Eqs. (2.1) and (2.2) we obtain, after linearizing,

$$\frac{\partial A}{\partial t} = \delta \frac{\partial^2 A}{\partial x^2} - \phi \frac{\partial A}{\partial x} + a_{11} A + a_{12} B, \tag{2.5}$$

$$\frac{\partial B}{\partial t} = \frac{\partial^2 B}{\partial x^2} - r\phi \frac{\partial B}{\partial x} + a_{21} A + a_{22} B, \tag{2.6}$$

where $a_{11} = \partial f / \partial a$, $a_{12} = \partial f / \partial b$, $a_{21} = \partial g / \partial a$, and $a_{22} = \partial g / \partial b$ are evaluated at S.

The conditions for spatiotemporal instability are satisfied when the spectrum of the linearized operator for the system (2.5), (2.6) enters the right-hand plane. Using the exponential solution ansatz $A, B \sim \exp[\omega t + ik(\omega)x]$, where ω is the eigenvalue and k is the wave number of the perturbation, and substituting into Eqs. (2.5) and (2.6) gives the *dispersion relation*

$$\begin{aligned} D(\omega, k) = {} & \omega^2 + [(1+\delta)k^2 - Tr + ik\phi(1+r)]\omega + \delta k^4 \\ & + i\phi k^3 (1 + r\delta) - k^2 (a_{11} + \delta a_{22} + r\phi^2) \\ & - ik\phi (r a_{11} + a_{22}) + \Delta, \end{aligned} \tag{2.7}$$

where

$$Tr = a_{11} + a_{22} < 0, \quad \Delta = a_{11} a_{22} - a_{12} a_{21} > 0. \tag{2.8}$$

Equation (2.8) implies that $\min\{a_{11}, a_{22}\} < 0$. Without restricting the generality we shall henceforth assume that $a_{11} < 0$. Clearly there are two main cases of instability possible through a primary bifurcation, namely, when $\omega = 0$, corresponding to a steady or FDS bifurcation (the Turing case is included), or when $\mathrm{Re}(\omega) = 0$, $\mathrm{Im}(\omega) \neq 0$, corresponding to a periodic solution (Hopf or DIFI bifurcation).

A. FDS instabilities

The FDS situation has been analyzed for some special cases before [1,3]. For the general case the critical FDS flow is given by

$$\phi_{FDS}^2 = -\frac{(1 + r^2\delta^2) a_{12} a_{21} + r(a_{11} - \delta a_{22})^2 + 2\delta a_{12} a_{21} r}{r(1 + r\delta)(a_{11} r + a_{22})} \tag{2.9}$$

for $r \neq 0$ and $r a_{11} + a_{22} \neq 0$. Generically, Eq. (2.9) has a strictly positive minimum ϕ_{FDS}^c, and the FDS instability is predicted for all $\phi \geqslant \max_{0 < r < -a_{22}/a_{11}} \{0, \phi_{FDS}\}$. This is similar to the Turing case which occurs in the domain $\delta \geqslant \delta_T > 1$ where δ_T is the critical Turing ratio of the diffusivities [3]. Space-periodic FDS waves have purely imaginary wave numbers $k_{FDS} = i z_{FDS}$, $z_{FDS} > 0$ given by

$$z_{FDS} = \sqrt{\frac{a_{11} r + a_{22}}{1 + r\delta}} > 0. \tag{2.10}$$

These exist only when $r < -a_{22}/a_{11}$. A more detailed analysis of the *neutral curve* (2.9) shows that $a_{22} > 0$ and $a_{12} a_{21} < 0$. Figures 1(a) and 1(b) show typical plots of the neutral curve (2.9) for kinetics (2.3). Another feature of the model is the relative insensitivity of the critical FDS value ϕ_{FDS}^c to variations in δ as shown in Fig. 1(a).

B. Differential-flow instability

The case $\mathrm{Re}(\omega) = 0$ in Eq. (2.7) leads to a Hopf bifurcation giving rise to space- and time-periodic traveling DIFI waves. The neutral curve $\phi_{DIFI}(k, \delta)$ that corresponds to bifurcation to spatiotemporal traveling DIFI solutions is

$$\begin{aligned} & \phi_{DIFI}^2(k^2, \delta, f, g) \\ & \quad = \frac{[\delta k^4 - (a_{11} + \delta a_{22}) k^2 + \Delta][(1+\delta)k^2 - Tr]^2}{(r-1)^2 (a_{22} - k^2)(\delta k^2 - a_{11}) k^2} \end{aligned} \tag{2.11}$$

for $r \neq 1$, $a_{22} - k^2 \neq 0$, $a_{11} - \delta k^2 \neq 0$. From Eq. (2.11) we recover the previously published results for the cases when $\delta = 0$, $r = 1$, and for the ionic model [11].

A detailed analysis of the neutral curve (2.11) shows that the differential-flow instability occurs for any $r \neq 1$ as follows. In the FDS regime $0 \leqslant \delta \leqslant \delta_T$, necessary conditions for instability are that $a_{11} a_{22} < 0$ and $a_{12} a_{21} < 0$. Let $\phi_{DIFI}^c > 0$ be the minimum of the neutral function (2.11) [see Fig. 1(c)]. In this case we require that $\phi \geqslant \phi_{DIFI} \geqslant \phi_{DIFI}^c > 0$. In the Turing regime $\delta > \delta_T$ we have $\phi_{DIFI}^c < 0$, and for instability we require that $\phi \geqslant \max\{0, \phi_{DIFI}\}$. In our case traveling waves are predicted even if differential diffusion is not present in the system, i.e., for $\delta = 1$, which is an unusual property for models of differential-flow instability. Figure 1(c) shows a typical neutral DIFI curve for the model (2.1), (2.3) for the case $\delta = 1.0$, $r = 0.05$, $\mu = 3.0$ giving $\phi_{DIFI}^c = 21.65$.

C. The relation between FDS and DIFI instabilities

Our analysis shows that FDS and DIFI instabilities can occur simultaneously for $0 \leqslant r < -a_{22}/a_{11}$, $\phi \geqslant \max\{\phi_{DIFI}, \phi_{FDS}\}$. Then the FDS critical wave number (2.10) is in the range $0 < k_{FDS}^2 < a_{22}$. Since the DIFI condition $\mathrm{Re}(\omega) = 0$ is guaranteed at the neutral FDS boundary $\omega = 0$ we find from Eqs. (2.9) and (2.11) that

$$\phi_{FDS}^2 = \phi_{DIFI}^2(k_{FDS}^2) \geqslant \min_{0 < k^2 < a_{22}} \phi_{DIFI}^2 = (\phi_{DIFI}^c)^2. \tag{2.12}$$

Hence the two neutral curves are always tangent at k_{FDS}. In particular, the DIFI instability is always generated first as the flow rate ϕ is increased from 0 to large values. We have explored these predictions numerically for the system (2.3). The result is given in Fig. 1(d). $\delta = 1.0$, $\mu = 3.0$ gives $-a_{22}/a_{11} = 0.11$. For $0 < r < 0.11$, as established above, $\phi_{FDS} \geqslant \phi_{DIFI}$. In the range $0.042 < r < 0.055$ the critical flow values for FDS and DIFI are relatively close and the two critical wave numbers have similar magnitudes. As seen below [Fig. 2(c)] the stationary FDS waves dominate the behavior in this range. Outside this traveling and stationary

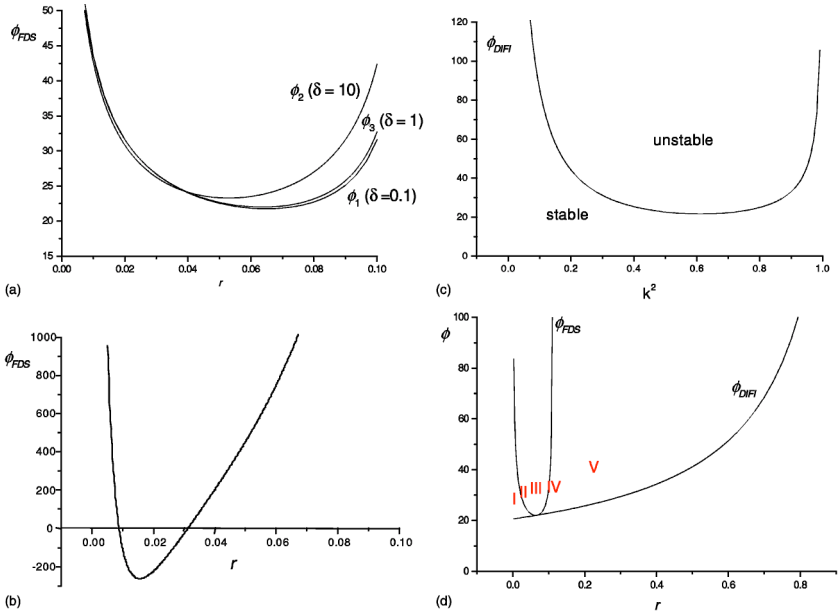

FIG. 1. Neutral FDS curves (2.9) for the cubic autocatalator model (2.3) for $\mu=3.0$ and (a) three different diffusion ratios $\delta=0.1,1,10$. (b) $\delta=60$. Here $\delta_T=(3+2\sqrt{2})\mu^2\approx 52.45$. (c) Neutral DIFI curve (2.11) for the cubic autocatalator system (2.3) as a function of k^2. Parameters: $\delta=1.0, r=0.05, \mu=3.0$. (d) Bifurcation diagram displaying the neutral FDS and DIFI flow curves for system (2.1), (2.3). Parameters: $\delta=1.0, \mu=3.0$. The regions with dynamical behavior as shown in Figs. 2(a)–2(d) below are labeled I–V. In region I there are only backward traveling waves. In region II, FDS and backward DIFI waves coexist. Region III has only FDS waves. In region IV, FDS and forward DIFI waves coexist. Region V has only forward traveling DIFI waves.

waves may coexist. Figure 1(d) also predicts that for values of r near a certain vicinity of zero or for r in a certain vicinity of 0.11 only traveling waves are expected (for such r's the difference $\phi_{FDS}-\phi_{DIFI}$ is very large). Finally note that for $r>0.11$ only DIFI waves are predicted with $\phi_{DIFI}\rightarrow\infty$ as $r\rightarrow 1^-$.

III. NUMERICAL SIMULATIONS

In order to illustrate our results we have explored numerically the spatiotemporal behavior of the model (2.3), using Fig. 1(d) as a guide to choosing parameters. The coupled parabolic system (2.1), (2.2) with reaction terms (2.3) was

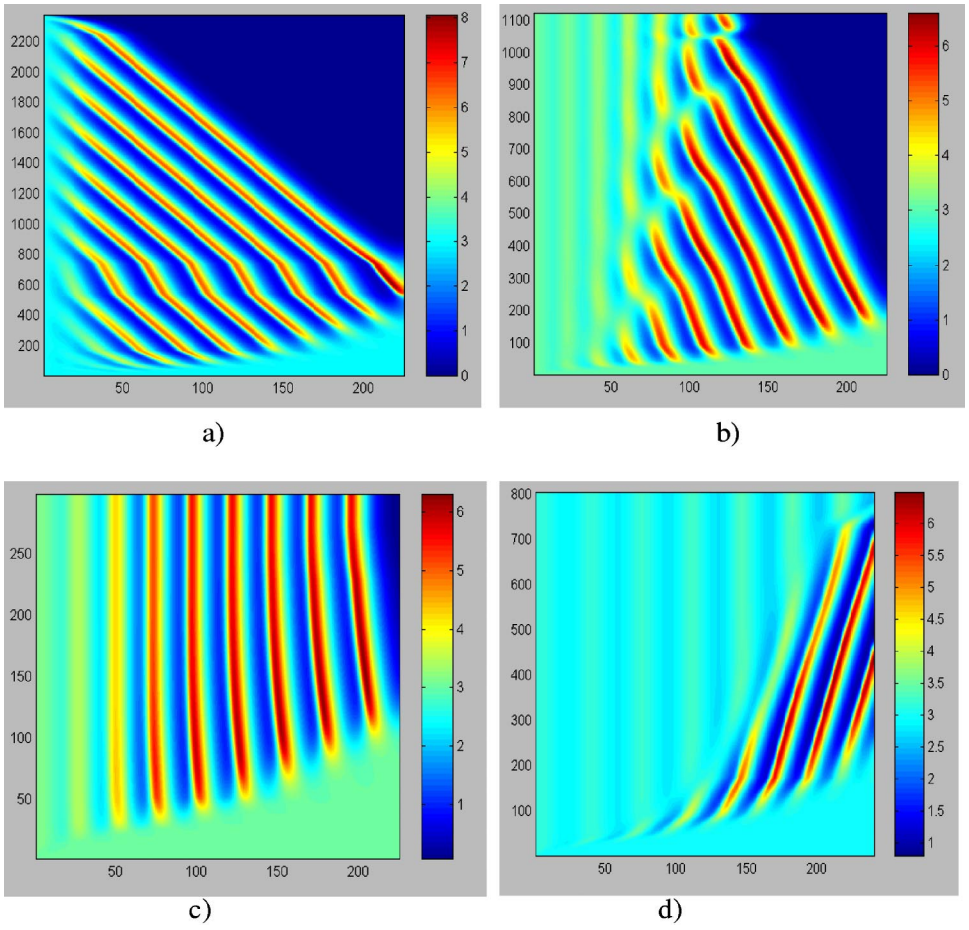

FIG. 2. Space-time contour plots of autocatalyst density b for the case $\mu=3.0, \delta=1.0, \phi=30.0$. Space is horizontal and time vertical. (a) $r=0.01$. Initially, periodic upstream traveling DIFI waves are formed. However, this structure is not stable and at $t\sim 600$ an extinct state (zero autocatalyst or $b\sim 0$) invades the entire domain. (b) $r=0.029$. A new stable structure of stationary space-periodic FDS waves appears behind the leading traveling waves. It remains stable and is not destroyed by the zero autocatalyst state. (c) $r=0.04$. The only nonuniform patterns are stationary FDS waves. The extinct state is confined to a small region near the outflow boundary. (d) $r=0.09$. Traveling DIFI and stationary FDS waves coexist in a stable manner.

integrated using an implicit Crank-Nicolson code with variable time stepping [3,11]. At the inflow $x=0$ we used a Dirichlet boundary condition in the form of a constant deviation from the uniform steady state S. At the outflow $x=L$ we used the free boundary condition $\partial^2 a/\partial x^2 = \partial^2 b/\partial x^2 = 0$. The system was left to evolve for a sufficient long time for a permanent structure to be established in the full computational domain.

For the reaction kinetics (2.3) we have $\delta_T=(3+2\sqrt{2})\mu^2$ (see [1,11]). Typical results for the case $0<\delta\leqslant\delta_T$ are shown in Figs. 2(a)–2(d) for representative parameter values. Consistent with our analytical predictions [Fig. 1(a)] the critical flow ϕ_{FDS} is not sensitive to variations in δ. For simulations it was fixed to $\delta=1$. On the other hand, ϕ_{FDS} depends sensitively on r, the differential-flow rate, as expected from the above analysis. For Figs. 2(a)–2(d) we fixed $\mu=3.0$ and $\phi=30.0\geqslant\phi_{FDS}^c\approx 22.0$ [see also Fig. 1(d)]. Figure 2(a) shows a contour plot of the autocatalyst density profile for $r=0.01$. Following the initial sequential propagation of the perturbation in the domain, periodic upstream traveling DIFI waves establish themselves. However, at about $t\sim 600$ an extinct state with zero autocatalyst ($b\sim 0$) begins to invade the whole domain at the outflow boundary. This picture is valid for all r sufficiently small and $0<\delta<\delta_T$. These waves moving against the flow are interesting especially when compared with previous studies [11] which showed that a DIFI bifurcation is associated with a convective instability at least when the uniform stationary state is stable as is the present case. As r is increased further, the traveling waves become increasingly unstable and split into two parts. The region close to the inflow boundary develops into stationary FDS waves [Fig. 2(b)]. Between approximatively $r=0.04$ and 0.055 only stable stationary waves are formed [Fig. 2(c)]. For $0.095\geqslant r\geqslant 0.6$ there is again a structure composed of two sections, illustrated by Fig. 2(d), with the front part forming downstream propagating high amplitude DIFI waves and the rear section settling into stationary, low amplitude FDS waves as $t\to\infty$. Finally, for $r\geqslant -a_{22}/a_{11}\approx 0.11$, only downstream propagating DIFI waves survive, forming a transient structure in the domain due to the convective instability of the uniform steady state (not shown). The overall picture is much the same in the Turing domain where $\delta>\delta_T=(3+2\sqrt{2})\mu^2$.

Further study shows that the above wave behavior is a robust and generic feature among a wide class of autocatalytic coupled systems of RDA that are widely employed in biological and chemical modeling. In all cases we found that similar waves arise in systems with the Belousov-Zhabotinskii (BZ) Oregonator [12], FitzHugh-Nagumo [13], and CIMA [14] kinetics. In the BZ-Oregonator case we found traveling waves that accelerate and decelerate (jump). These results will be given elsewhere [15].

ACKNOWLEDGMENT

I thank Michael Menzinger (Toronto) for many useful discussions.

[1] R. A. Satnoianu and M. Menzinger, Phys. Rev. E **62**, 113 (2000).
[2] A. B. Rovinsky and M. Menzinger, Phys. Rev. Lett. **70**, 778 (1993).
[3] R. A. Satnoianu, P. K. Maini, and M. Menzinger, Physica D **160**, 79 (2001).
[4] A. M. Turing, Philos. Trans. R. Soc. London, Ser. B **237**, 37 (1952).
[5] P. Andresen, M. Bache, E. Mosekilde, G. Dewel, and P. Borckmans, Phys. Rev. E **60**, 297 (1999).
[6] M. Kaern and M. Menzinger, Phys. Rev. E **60**, 3471 (1999).
[7] O. A. Nekhamkina, A. A. Nepomnyashchy, B. Y. Rubinstein, and M. Sheintuch, Phys. Rev. E **61**, 2436 (2000); O. Nekhamkina and M. Sheintuch, *ibid.* **66**, 016204 (2002).
[8] J. R. Bamforth, J. H. Merkin, S. K. Scott, R. Toth, and V. Gaspar, Phys. Chem. Chem. Phys. **3**, 1435 (2001).
[9] P. V. Kuptsov, S. P. Kuznetsov, and E. Mosekilde, Physica D **163**, 80 (2002).
[10] M. Kaern, M. Menzinger, and A. Hunding, J. Theor. Biol. **207**, 473 (2000); M. Kaern, M. Menzinger, R. A. Satnoianu, and A. Hunding, Faraday Discuss. **120**, 295 (2001).
[11] R. A. Satnoianu, J. H. Merkin, and S. K. Scott, Physica D **124**, 354 (1998); J. H. Merkin, R. A. Satnoianu, and S. K. Scott, Dyn. Stab. Syst. **15**, 209 (2000).
[12] B. P. Belousov, in *Oscillations and Traveling Waves in Chemical Systems*, edited by R. J. Field and M. Burger (Wiley, New York, 1985); A. M. Zhabotinskii, Biofizika **9**, 306 (1964).
[13] J. S. Nagumo, S. Arimoto, and S. Yoshizawa, Proc. IRE **50**, 2061 (1962); R. FitzHugh, Biophys. J. **1**, 445 (1961).
[14] I. Lengyel and I. Epstein, Science **251**, 650 (1991).
[15] R. A. Satnoianu and M. Menzinger (unpublished).